# Circuit Model for Periodic Array of Slits With Multiple Propagating Diffracted Orders

Elahe Yarmoghaddam, Ghazaleh Kafaie Shirmanesh, Amin Khavasi, and Khashayar Mehrany

***Abstract*—We propose an analytical circuit model for accurate analysis of one-dimensional periodic array of metallic strips. The proposed model is valid not only in subwavelength regime, but also for wavelengths shorter than the period of structure. The working frequency can reach the visible range and thus electromagnetic properties of periodic arrays of nano-slits can be analyzed by the proposed model. The proposed model remains valid for arbitrary incident angles even when nonspecular diffracted orders become propagating. Analytical expressions are derived explicitly in order to describe the parameters of the proposed circuit model. The circuit model is derived by assuming that only one guided mode is supported by the slits. The model can successfully explain the extraordinary transmission phenomenon from microwave to optical frequencies. The circuit model is presented for both major polarizations.**

***Index Terms*—Circuit model, extraordinary transmission, metallic grating, nano-slit arrays.**

## I. Introduction

EXTRAORDINARY transmission (EOT) has been a hot topic for researches since its discovery [1]. Unusual electromagnetic responses such as EOT have been observed in periodic metallodielectric structures [2]. These structures have been investigated using numerical methods, namely finite difference time domain (FDTD) [3], finite integration techniques [4], and finite element method. However, these methods are very time consuming and give no insight to the subject. Recently, analytical methods have been developed to analyze metallic gratings. One of these analytical approaches is to use equivalent circuit models that let us design and analyze periodic structures more easily and quickly. Circuit models are also useful for providing an alternative understanding of important phenomena such as EOT [5], [6]. They enable us to explain the EOT in the sub-wavelength regime by using the impedance matching concept. Previously, equivalent circuit models have been presented for different periodic metallic structures including two-dimensional array of holes [5] and one-dimensional array of slits [7]. In [7], the grating region is modeled by a transmission line to account for the TEM mode propagating inside the slits which is terminated to a capacitor modeling the effect of the evanescent diffracted orders. Nevertheless, in this model some essential parameters are not explicitly given in closed form expressions. Moreover, the validity of the proposed model is limited to normal incidence condition. Besides, this model is limited to the cases in which the region above the grating is free space. The mentioned problem was obviated in [8] in such a way that the employed 1-D metallic grating was sandwiched between two dielectric slabs with arbitrary indices of refraction, illuminated by TM-polarized electromagnetic wave. In [2], considering the stated obstacles has yielded to further improvement of the equivalent circuit model for such 1-D metallic gratings. This model has two benefits: one is that it remains valid at arbitrary incident angles, and the other is that all its parameters are given by closed form expressions. Despite the progress that has been hitherto made, the expressions used for capacitors in the above-mentioned models are empirically obtained by using results of full-wave simulations. Moreover, the validity of the models is limited to the sub-wavelength regime, i.e., when all nonspecular orders are below cutoff and there is only one propagating diffracted order (the specular one) outside the grating region.

In this paper, we propose a fully analytical circuit model for the array of slits perforated in the metallic slabs to be used at the frequencies at which higher diffracted orders can be propagating. For TM polarization, our method is based on replacing the capacitor in [2] with infinite number of parallel capacitors, each representing a specific diffracted order. When a diffracted order becomes propagating, its equivalent capacitor is converted to a resistor. We illustrate that power loss in each resistor is equal to the power transmitted to its corresponding diffracted order. All the parameters of the proposed circuit model are given by analytical expressions. The circuit model is also extended to the TE polarization, but in this case the capacitors should be replaced by inductors. This method is also valid for different incident angles, and it is relatively accurate up to visible range. The circuit model is derived by assuming that the non-principal guided modes of the slit are below cutoff. We verify the accuracy of the proposed model by comparing it with full-wave numerical simulations. There is an excellent agreement between the results of the proposed analytical model and the numerical method.

The paper is organized as follows. In Section II, the proposed circuit model for periodic array of metallic slits is introduced. In Section III, we extend our model to visible range. Simulation results are then given in Section IV, and Section V concludes the paper.

Manuscript received October 24, 2013; revised February 16, 2014; accepted April 02, 2014. Date of publication May 09, 2014; date of current version July 31, 2014.

The authors are with the Electrical Engineering Department, Sharif University of Technology, Tehran 11155-4363, Iran (e-mail: e_yarmoghaddam@ee.sharif.edu; kafaie@ee.sharif.edu; khavasi@sharif.edu; mehrany@sharif.edu).

Color versions of one or more of the figures in this paper are available online at http://ieeexplore.ieee.org.

Digital Object Identifier 10.1109/TAP.2014.2322884

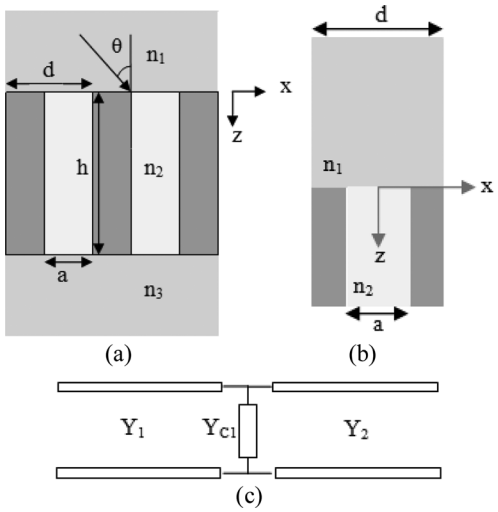


Fig. 1. (a) Periodic array of metallic strips under the incidence of a uniform plane wave. (b) The structure with two semi-infinite regions: homogenous medium and the metallic grating, used for extracting the shunt admittance modeling the effect of the two regions' interface. (c) Equivalent circuit model for the structure depicted in (b).

## II. Circuit Model

In this section, we present our analytical circuit model for periodic arrays of slits perforated in metallic slabs. We first drive our model for working in low frequency regime, where the metallic region can be approximated by perfect electric conductor (PEC). Then in the next section, we extend our model to the visible range by taking the plasmonic behavior of metals into account.

Consider a periodic array of metallic slits filled with a dielectric medium whose refractive index is $n_2$ and is sandwiched between two homogenous regions with refractive indices of $n_1$ and $n_3$. Fig. 1(a) illustrates the structure under study, with $d$ being the period of the structure, $h$ the thickness of the metal plate, and $a$ the spacing between the metallic strips.

First, for the sake of simplicity, we assume that the grating region is semi-infinite ($h \to \infty$) as depicted in Fig. 1(b), to extract the shunt admittance which models the effect of higher order diffracted waves at the interface of the grating region and the homogenous medium. Afterwards we extend our model to the structure shown in Fig. 1(a).

### A. TM Polarization

Assume that the structure is illuminated by a TM polarized wave (the magnetic field in $\hat{y}$ direction) whose incidence angle is $\theta$. The magnetic and tangential electric fields of the incident wave in region 1 are (the time dependence of $e^{j\omega t}$ is assumed here)

$$E_{1x} = E_{10}^{+}e^{-jk_{x10}x}e^{-jk_{z10}z} + E_{10}^{-}e^{-jk_{x10}x}e^{+jk_{z10}z} + \sum_{m\neq 0} E_{1m}^{-}e^{-jk_{x1m}x}e^{+jk_{z1m}z} \quad (1a)$$

$$H_{1y} = \xi_{10}\left(E_{10}^{+}e^{-jk_{z10}z} - E_{10}^{-}e^{+jk_{z10}z}\right)e^{-jk_{x10}x} - \sum_{m\neq 0} \xi_{1m}E_{1m}^{-}e^{-jk_{x1m}x}e^{+jk_{z1m}z} \quad (1b)$$

where the superscript $(+)$ relates to the wave propagation in $\hat{z}$ direction, and superscript $(-)$ relates to the propagation in opposite direction. The first subscript (1) indicates the region where the fields are expanded. The second subscript corresponds to the order of the diffracted wave [9]. Besides, $k_{x1m}$ and $k_{z1m}$ are the wave-vector components in $\hat{x}$ and $\hat{z}$ directions in the first region and are given by

$$k_{x1m} = k_{x10} + \frac{2m\pi}{d}; \quad (m = 0, \pm 1, \pm 2, \ldots) \quad (2)$$

$$k_{z1m} = -jk_0\sqrt{\left(n_1\sin(\theta) + \frac{m\lambda}{d}\right)^2 - n_1^2}; \quad (m = 0, \pm 1, \pm 2, \ldots) \quad (3)$$

where

$$k_{x10} = k_0 n_1 \sin(\theta) \quad (4)$$

and $k_0 = 2\pi/\lambda$ is the wavenumber in free space, and $\lambda$ is the free space wavelength. The $z$ component of the wavevector, $k_{z1m}$ is either positive real (propagating wave) or negative imaginary (evanescent wave).

Moreover, in (1b),

$$\xi_{1m} = \omega\varepsilon_1/k_{z1m} \quad (5)$$

is the wave admittance of the $m'$th diffracted order in the region 1, where $\varepsilon_1$ is the permittivity of the first medium, and $\omega = 2\pi f$ is the angular frequency with $f$ being the frequency [9]. In region 2, by assuming that the slit is single mode, the electromagnetic fields are

$$E_{2x} = E_{20}^{+}e^{-j\beta_2 z} \quad (6a)$$

$$H_{2y} = \xi_{20}E_{20}^{+}e^{-j\beta_2 z}. \quad (6b)$$

Hence, the validity of the proposed circuit model is limited to the frequency range which is below the cutoff frequency of the first higher order mode inside the slits. This condition requires that $\lambda > 2an_2$ [2]. In (6), $\beta_2$ is the propagation constant of the TEM mode supported by a parallel plate waveguide and is obtained by

$$\beta_2 = k_0 n_2. \quad (7)$$

Furthermore, the wave admittance of medium 2 with permittivity $\varepsilon_2$ is given by

$$\xi_{20} = \frac{\omega\varepsilon_2}{\beta_2}. \quad (8)$$

By applying the standard boundary conditions at $z = 0$, i.e., the continuity of the tangential electric field at every point of unit cell and continuity of the tangential magnetic field at slit locations, the reflection coefficient of the structure can be obtained as follows.

Applying the continuity of the tangential electric fields, by using (1a) and (6a), leads to the following relations:

$$(E_{10}^{+} + E_{10}^{-}) = E_{20}^{+}\frac{\sin\left(\frac{k_{x10}a}{2}\right)}{d\frac{k_{x10}}{2}} \quad (9)$$

$$E_{1m}^{-} = E_{20}^{+}\frac{\sin\left(\frac{k_{x1m}a}{2}\right)}{d\frac{k_{x1m}}{2}} \quad (10)$$

which are obtained by multiplying the electric fields to $e^{jk_{x1m}x}$ and taking the integral of both sides over one period.

Similarly, applying the continuity of the tangential magnetic fields by using (1b) and (6b), and taking the integral of both side over one slit width, leads to

$$\xi_{10}(E_{10}^{+}-E_{10}^{-})-\sum_{m\neq 0}\xi_{1m}E_{1m}^{-}A_{1m} = \xi_{20}E_{20}^{+}\left(\frac{k_{x10}a/2}{\sin(k_{x10}a/2)}\right) \quad (11)$$

where

$$A_{1m}=\frac{\sin(k_{x1m}a/2)}{k_{x1m}a/2}\frac{k_{x10}a/2}{\sin(k_{x10}a/2)}. \quad (12)$$

Now combining (9), (10) and (11) we have the reflection coefficient of the zeroth (specular) diffracted order

$$\Gamma_0=\frac{E_{10}^{-}}{E_{10}^{+}}=\frac{\left(\xi_{10}-\xi_{20}\frac{d}{a}\left(\frac{k_{x10}a/2}{\sin(k_{x10}a/2)}\right)^2-\sum_{m\neq 0}\xi_{1m}A_{1m}^2\right)}{\left(\xi_{10}+\xi_{20}\frac{d}{a}\left(\frac{k_{x10}a/2}{\sin(k_{x10}a/2)}\right)^2+\sum_{m\neq 0}\xi_{1m}A_{1m}^2\right)}. \quad (13)$$

Equation (13) resembles the reflection coefficient in the circuit shown in Fig. 1(c), which is given by [9]

$$\Gamma=\frac{Y_1-[Y_2+Y_{C1}]}{Y_1+[Y_2+Y_{C1}]}. \quad (14)$$

Comparison of (13) and (14) gives $Y_1=\xi_{10}$ and

$$Y_2=\xi_{20}\frac{d}{a}\left(\frac{k_{x10}a/2}{\sin(k_{x10}a/2)}\right)^2 \quad (15)$$

which are corresponding to the characteristic admittances of regions 1 and 2, respectively [9]. It is worth noticing that for normal incidence the expression given for the admittance of the grating region in the previous works is recovered [7], [2]. However, for nonzero incident angles the equivalent admittance should be corrected as presented in this work.

In (14), $Y_{C1}$ that accounts for the evanescent fields on the surface of the structure [9], is given by

$$Y_{C1}=\sum_{m\neq 0}\xi_{1m}A_{1m}^2=\sum_{m\neq 0}\frac{\omega\varepsilon_1}{k_{z1m}}A_{1m}^2 \quad (16)$$

Therefore, $Y_{C1}$ can be considered as infinite number of parallel capacitors each of them is calculated by

$$C_1^m=\frac{\varepsilon_1}{jk_{z1m}}A_{1m}^2 \quad (17)$$

where $C_1^m$ is the capacitor corresponding to the $m'$th diffracted order, and according to (17) when the $m'$th diffracted order becomes propagating, its corresponding capacitance becomes pure imaginary and turns out to a resistor. We demonstrate that the power dissipated in each resistor is equal to the power transmitted to its corresponding diffracted order. To substantiate this, first, we assume that $m'$th diffracted order has become propagating; therefore, $C_1^m$ is changed to $R_1^m=1/j\omega C_1^m$; then we calculate the normalized power dissipated in $R_1^m$, and we show that it is equal to the diffraction efficiency of the $m'$th diffracted order.

The voltage and current on the left transmission line in the equivalent circuit are obtained by [10]

$$V_1=V_1^{+}e^{-j\beta z}+V_1^{-}e^{+j\beta z} \quad (18a)$$
$$I_1=I_1^{+}e^{-j\beta z}+I_1^{-}e^{+j\beta z} \quad (18b)$$

where $I_1^{\pm}=\pm Y_1V_1^{\pm}$ and $V_1^{-}=\Gamma V_1^{+}$. Hence, the incident power is

$$P_{\text{incident}}=\frac{1}{2}\text{Re}(V_1^{+}I_1^{+*})=\frac{1}{2}|Y_1V_1^{+}|^2\text{Re}\left(\frac{1}{Y_1}\right). \quad (19)$$

Furthermore, the voltage across $R_1^m$ is

$$V_R=V_1|_{z=0}=V_1^{+}(1+\Gamma) \quad (20)$$

and thus the power dissipated in $R_1^m$ can be easily calculated as

$$P_R=\frac{1}{2}\left|\frac{V_R}{R_1^m}\right|^2R_1^m=\frac{1}{2}\left|\frac{V_1^{+}(1+\Gamma)}{R_1^m}\right|^2R_1^m \quad (21)$$

and finally the normalized power dissipated in $R_1^m$ is

$$P_{\text{normalized}}=\frac{P_R}{P_{\text{incident}}}=\frac{R_1^m}{\text{Re}\left(\frac{1}{Y_1}\right)}\left|\frac{1}{Y_1R_1^m}(1+\Gamma)\right|^2. \quad (22)$$

Substituting $R_1^m$ and $Y_1$ and after some simplifications we have

$$P_{\text{normalized}}=\left|\frac{k_{z10}}{k_{z1m}}A_{1m}(1+\Gamma)\right|^2\text{Re}\left(\frac{k_{z1m}}{k_{z10}}\right). \quad (23)$$

On the other hand, the diffraction efficiency which is the ratio of the diffracted power to the incident one is [11]

$$DE_{rm}=\Gamma_m\Gamma_m^{*}\text{Re}\left(\frac{k_{z1m}}{k_{z10}}\right) \quad (24)$$

where $\Gamma_m$ is the reflection coefficient of the $m'$th reflected order which is obtained from (9) and (10), and (13):

$$\Gamma_m=\frac{\xi_{1m}}{\xi_{10}}A_{1m}(1+\Gamma_0). \quad (25)$$

Accordingly, $DE_{rm}$ is simplified to

$$DE_{rm}=\left|\frac{k_{z10}}{k_{z1m}}A_{1m}(1+\Gamma_0)\right|^2\text{Re}\left(\frac{k_{z1m}}{k_{z10}}\right). \quad (26)$$

Therefore, power dissipated in $R_1^m$ is obviously equal to the diffraction efficiency of the $m'$th diffracted order.

Now, we can present appropriate circuit model (Fig. 2) for the structure shown in Fig. 1(a). In this circuit, $Y_3=\xi_{30}$ and $Y_{C3}=\sum_{m\neq 0}\xi_{3m}A_{3m}^2$ where $\xi_{30}$ and $A_{3m}$ are obtained using (5) and (12), respectively, by substituting the corresponding parameters of the third region, and other parameters have been already given.

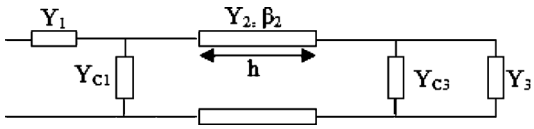


Fig. 2. Proposed circuit model for the structure shown in Fig. 1(a).

### B. TE Polarization

For obtaining the circuit model for TE polarization, similar to the TM polarization, at first, we define the electric and magnetic fields in each region. In region 1, the electric and magnetic fields are given as

$$E_{1y} = E_{10}^{+}e^{-jk_{x10}x}e^{-jk_{z10}z} + E_{10}^{-}e^{-jk_{x10}x}e^{+jk_{z10}z} + \sum_{m\neq 0} E_{1m}^{-}e^{-jk_{x1m}x}e^{+jk_{z1m}z} \tag{27a}$$

$$H_{1x} = \xi_{10}\left(-E_{10}^{+}e^{-jk_{z10}z} + E_{10}^{-}e^{+jk_{z10}z}\right)e^{-jk_{x10}x} + \sum_{m\neq 0} \xi_{1m}E_{1m}^{-}e^{-jk_{x1m}x}e^{+jk_{z1m}z} \tag{27b}$$

where

$$\xi_{1m} = k_{z1m}/\omega\mu \tag{28}$$

is the wave admittance of $m'$th diffracted order in region 1.

In region 2, by assuming that there is only the first TE mode of the parallel plate waveguide, the electromagnetic fields are

$$E_{2y} = E_{20}^{+}\sin\left(\frac{\pi x}{a}\right)e^{-j\beta_2 z} \tag{29a}$$

$$H_{2x} = -\xi_{20}E_{20}^{+}\sin\left(\frac{\pi x}{a}\right)e^{-j\beta_2 z}. \tag{29b}$$

In this case, the validity of the proposed circuit model is limited to the frequency range below the cutoff frequency of the $\mathrm{TE}_2$ mode inside the slits. This condition requires that $\lambda > an_2$ [10]. In (29), $\beta_2$ is the propagation constant of the first TE mode supported by a parallel plate waveguide and is obtained by

$$\beta_2 = \sqrt{(k_0 n_2)^2 - \left(\frac{\pi}{a}\right)^2}. \tag{30}$$

Furthermore, the wave admittance of medium 2 is given by

$$\xi_{20} = \beta/\omega\mu. \tag{31}$$

Like the TM polarization, applying the continuity of the tangential electric field at $z = 0$ and multiplying the equation by $e^{jk_{x1m}x}$ and taking the integral of both sides over one period, leads to

$$(E_{10}^{+} + E_{10}^{-})d = E_{20}^{+}B_{10} \tag{32}$$

$$E_{1m}^{+}d = E_{20}^{+}B_{1m} \tag{33}$$

where

$$B_{1m} = \int_0^a e^{jk_{x1m}x}\sin\left(\frac{\pi x}{a}\right)d_x = -\frac{a\pi(1+e^{jk_{x1m}a})}{(k_{x1m}a)^2 - \pi^2}. \tag{34}$$

Similarly, applying the continuity of the tangential magnetic field at $z = 0$ and multiplying the equation by $\sin(\pi x/a)$ and taking the integral of both sides over one slit width, we have

$$\xi_{10}(-E_{10}^{+} + E_{10}^{-})D_{10} + \sum_{m\neq 0}\xi_{1m}E_{1m}^{-}D_{1m} = -\xi_{20}E_{20}^{+}\frac{a}{2} \tag{35}$$

where $D_{1m}$ is

$$D_{1m} = \int_0^a e^{-jk_{x1m}x}\sin\left(\frac{\pi x}{a}\right)d_x = -\frac{2a\pi e^{-jk_{x1m}\frac{a}{2}}\cos\left(k_{x1m}\frac{a}{2}\right)}{(k_{x1m}a)^2 - \pi^2}. \tag{36}$$

By using (32), (33), and (35), the reflection coefficient of the zeroth (specular) diffracted order can be written as

$$\Gamma_0 = \frac{E_{10}^{-}}{E_{10}^{+}} = \frac{\left(\xi_{10} - \xi_{20}\frac{ad}{2}\frac{1}{B_{10}D_{10}} - \sum_{m\neq 0}\xi_{1m}\frac{B_{1m}D_{1m}}{B_{10}D_{10}}\right)}{\left(\xi_{10} + \xi_{20}\frac{ad}{2}\frac{1}{B_{10}D_{10}} + \sum_{m\neq 0}\xi_{1m}\frac{B_{1m}D_{1m}}{B_{10}D_{10}}\right)}. \tag{37}$$

Comparison of (37) and (14) gives $Y_1 = \xi_{10}$ and

$$Y_2 = \xi_{20}\frac{d}{a}\frac{\pi^2}{8} \tag{38}$$

$$Y_{c1} = \sum_{m\neq 0}\xi_{1m}\frac{B_{1m}D_{1m}}{B_{10}D_{10}}. \tag{39}$$

$Y_{C1}$ can be considered as a series of infinite number of parallel inductors whose inductance is

$$L_1^m = \frac{\mu}{jk_{z1m}}\frac{B_{10}D_{10}}{B_{1m}D_{1m}}. \tag{40}$$

Similar to the TM case, when the $m'$th diffracted order becomes propagating, its corresponding inductance becomes pure imaginary and turns out to a resistor.

## III. Extension to the Visible Range

In the previous section, we obtained our model for working in low frequency regime; accordingly, we approximated metallic strips by PEC. Nevertheless, if the wavelength of incident plane wave becomes smaller and close to near infrared and optical ranges, our model is not valid. To extend our model to the mentioned frequency ranges, we have to modify the propagation constant of the grating region. We do this by considering the propagation constant of MIM waveguide ($\beta$) whose metal has a complex permittivity obtained from Drude model calculated by [12]

$$\varepsilon_m(\omega) = \varepsilon_\infty - \frac{\omega_p^2}{\omega^2 - i\omega\gamma} \tag{41}$$

where $\varepsilon_\infty$ is dielectric constant, $\omega$ is angular frequency, $\omega_p$ is plasma frequency of the free electron gas, and $\gamma$ is characteristic collision frequency. The sought-after propagation constant is

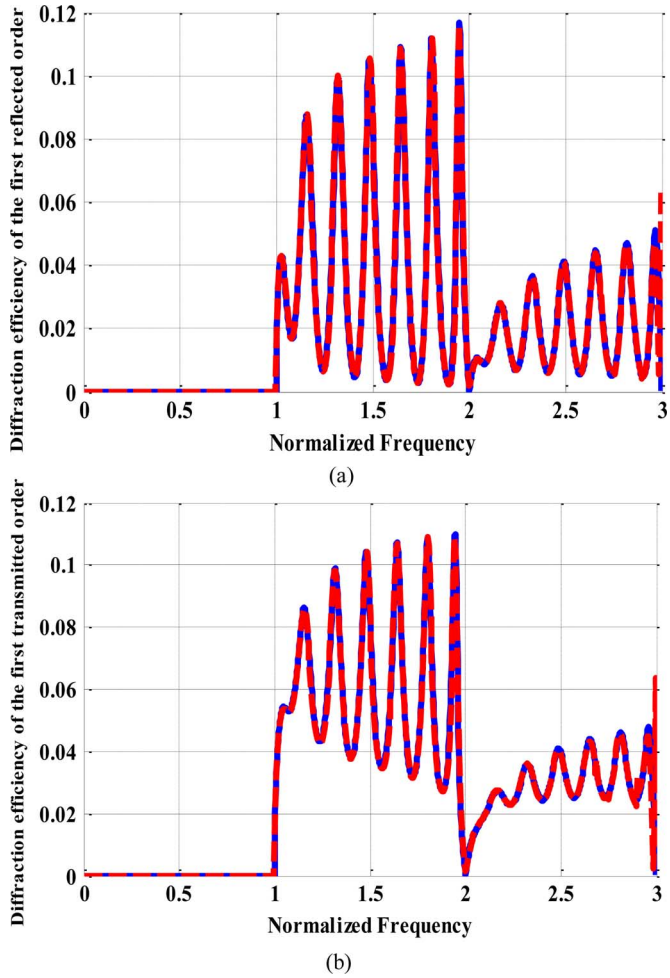


Fig. 3. (a) Diffraction efficiency of the first reflected order obtained by using rigorous full wave solution [13], [14] (dashed line), power dissipated in $R_1^1$ calculated by using proposed circuit model (solid line). (b) The diffraction efficiency of the first transmitted order obtained by using rigorous full wave solution [13], [14] (dashed line), power dissipated in $R_3^1$ resulted by using proposed circuit model (solid line), versus normalized frequency at normal incidences. The grating parameters are: $n_1 = n_3 = 1, n_2 = 2, d = 200\ \mu$m, $a = 40\ \mu$m, and $h = 300\ \mu$m. The grating illuminated by a TM polarized incident plane wave.

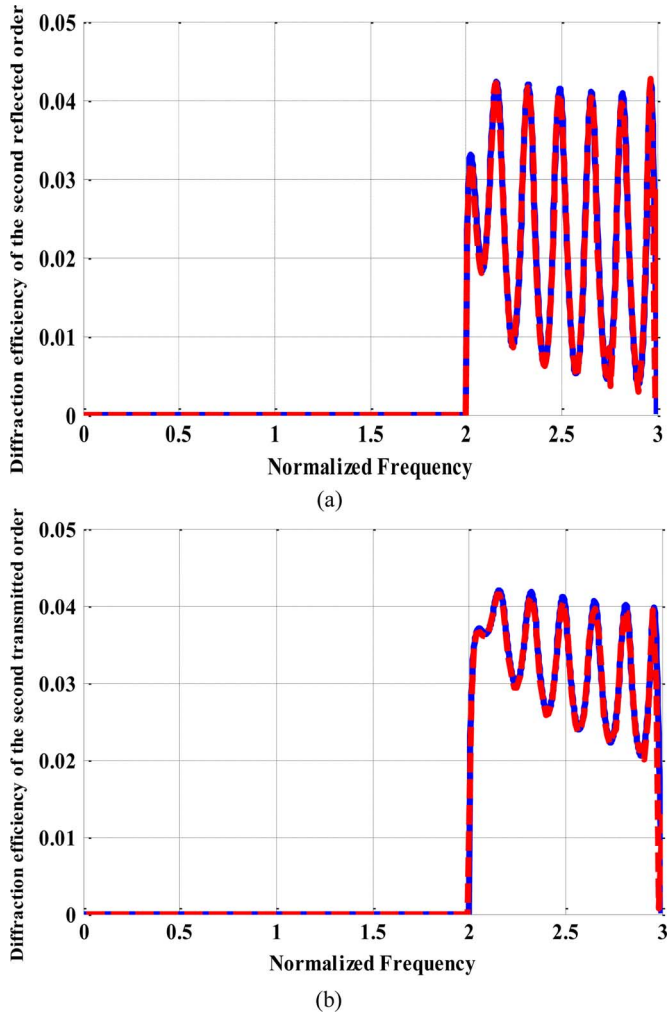


Fig. 4. (a) Diffraction efficiency of the second reflected order obtained by using rigorous full wave solution [13], [14] (dashed line), power dissipated in $R_1^2$ calculated by using proposed circuit model (solid line). (b) The diffraction efficiency of the second transmitted order obtained by using rigorous full-wave solution [13], [14] (dashed line), power dissipated in $R_3^2$ resulted by using proposed circuit model (solid line), versus normalized frequency at normal incidence. The grating parameters are: $n_1 = n_3 = 1, n_2 = 2, d = 200\ \mu$m, $a = 40\ \mu$m, and $h = 300\ \mu$m. The grating illuminated by a TM polarized incident plane.

obtained by solving the nonlinear equation of (42). Note that we consider only fundamental odd mode which does not exhibit a cutoff for vanishing core layer thickness [12]:

$$\tanh\left(\frac{k_i a}{2}\right) = -\frac{k_m \varepsilon_i}{k_i \varepsilon_m} \tag{42}$$

where $\varepsilon_i$ and $\varepsilon_m$ are relative permittivity of the insulator and metal, respectively. Besides, $k_i$ and $k_m$ are equal to

$$k_X^2 = \beta^2 - k_0^2 \varepsilon_X; \quad X = i, m. \tag{43}$$

Note that other parameters of this circuit model are the same as to the model described in Section II. In this way, we can analyze electromagnetic properties of periodic arrays of nano-slits by the proposed model.

## IV. Simulation Results

In this section, the accuracy of the proposed model is verified through some numerical examples. For rigorous results stable implementation of Fourier modal method with adaptive spatial resolution is used [13], [14] which has been demonstrated its applicability from microwave frequencies [13] up to visible range [15]. This method solves Maxwell's equations rigorously, and its accuracy have been verified with experimental results [13]. For rigorous simulation of PEC, a conductor with sufficiently high conductivity ($\sigma = 3.6 \times 10^7$) is assumed.

As the first numerical example, in accordance with Fig. 1(a), we set $n_1 = n_3 = 1, n_2 = 2, d = 200\ \mu$m, $a = 40\ \mu$m, and $h = 300\ \mu$m. The diffraction efficiency of the first reflected order of the structure, when illuminated by a TM polarized normal incident plane wave is plotted in Fig. 3(a), which is obtained by using the rigorous full-wave solution of [13], [14] (dashed line), and by the proposed circuit model (solid line) versus the normalized frequency $\omega_n = d/\lambda$. When the first diffracted order becomes propagating (in this case, for $\omega_n > 1$), its equivalent capacitors ($C_1^1$ and $C_3^1$) convert to resistors ($R_1^1$ and $R_3^1$). Fig. 3(a) demonstrates that the diffraction efficiency of the first reflected order obtained by the rigorous approach virtually overlaps with the power dissipated in $R_1^1$; and the same

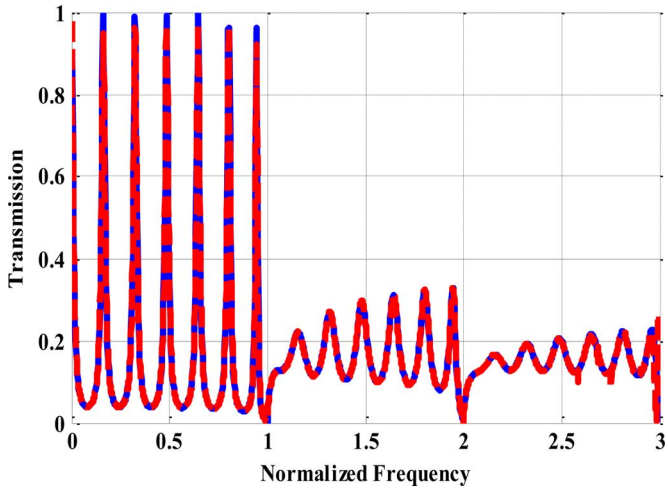


Fig. 5. Transmitted power through a grating illuminated by a TM polarized incident plane wave versus normalized frequency calculated by the rigorous approach of [13], [14] (dashed line), proposed circuit model (solid line). The structure parameters are: $n_1 = n_3 = 1, n_2 = 2, d = 200\ \mu$m, $a = 40\ \mu$m, and $h = 300\ \mu$m. The grating is under normal incidence.

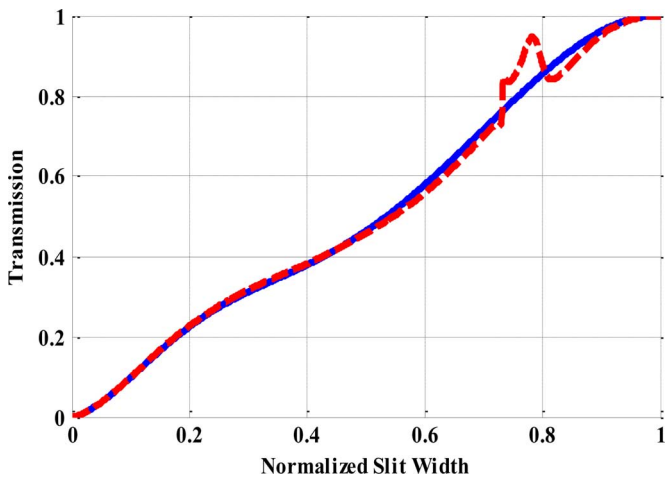


Fig. 6. Transmitted power through a grating illuminated by a TM polarized incident plane wave versus normalized slit width calculated by the rigorous approach of [13], [14] (dashed line), proposed model (solid line). The grating parameters are: $n_1 = n_2 = n_3 = 1, d = 200\ \mu$m, and $h = 300\ \mu$m. The grating is under normal incidence. The normalized frequency is $\omega_n = 1.4$.

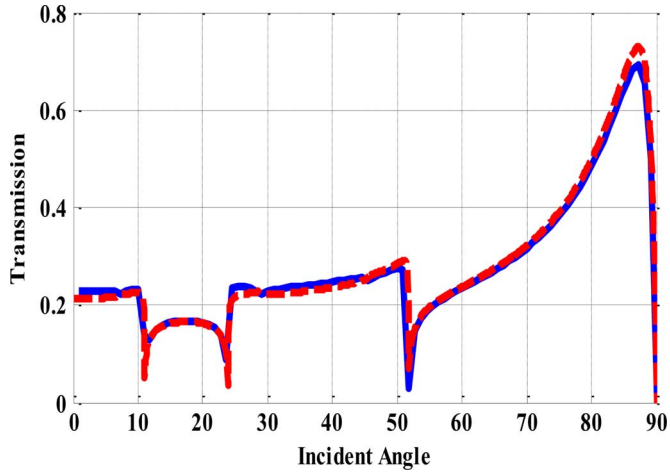


Fig. 7. Transmitted power through a grating illuminated by a TM polarized incident plane wave versus incident angle calculated by the rigorous approach of [13], [14] (dashed line) and the circuit model (solid line). The grating parameters are: $n_1 = 1.2, n_2 = 1.7, n_3 = 3, d = 200\ \mu$m, $a = 40\ \mu$m, and $h = 300\ \mu$m. The normalized frequency is $\omega_n = 1.4$.

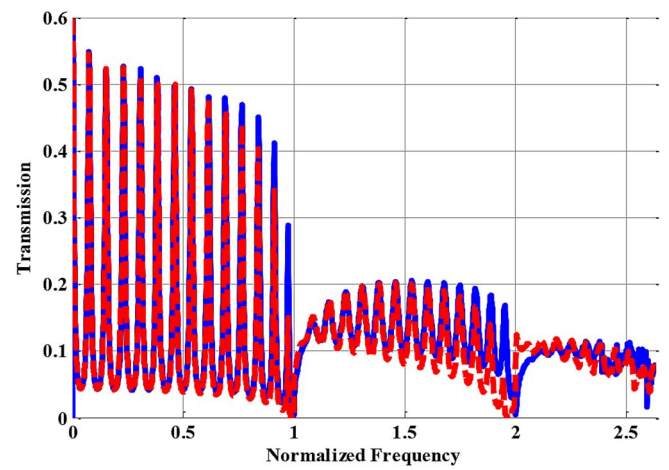


Fig. 8. Transmitted power through a grating illuminated by a TM polarized incident plane wave versus normalized frequency calculated by the rigorous approach of [13], [14] (dashed line) and proposed circuit model (solid line). The grating parameters are: $n_1 = n_3 = 1, n_2 = 2, d = 1\ \mu$m, $a = 0.2\ \mu$m, and $h = 3\ \mu$m. The grating is under normal incidence.

is true for the diffraction efficiency of the first transmitted order as depicted in Fig. 3(b). It is noticeable that in accordance with the period of the structure and the definition of the normalized frequency, the working frequency range is 0–4.5 THz.

In Fig. 4(a) and (b), the diffraction efficiencies of the second reflected and transmitted orders of the structure, when illuminated by the TM polarized normal incident plane wave, are plotted versus normalized frequency, respectively. Moreover, in Fig. 5, we have plotted the power transmission of the structure versus normalized frequency at normal incidence with consideration of all diffracted order. Excellent agreement is again observed. The results are obtained by using equivalent circuit model (solid line) and the rigorous approach of [13], [14] (dashed line).

The performance of the circuit model is also verified for different slit widths and incident angles. The transmitted power in the previous example is once again plotted versus the normalized slit width $(a/d)$ and incident angle in Figs. 6 and 7, respectively. The normalized frequency in these figures is $\omega_n = 1.4$ ($f = 2.1$ THz). The results obtained by using the proposed circuit model (solid line) is compared against those obtained by using the rigorous approach of [13], [14] (dashed line). It should be noticed that due to the excitation of higher order modes inside the slits for normalized slit width of larger than 0.714, the circuit model lose its accuracy as it is seen in Fig. 6.

Previous example was in low-frequency regime; now, for demonstrating the validity of our proposed model in the visible range, we set $n_1 = n_3 = 1, n_2 = 2, d = 1\ \mu$m, $a = 0.2\ \mu$m, and $h = 3\ \mu$m, and we consider Drude model for Aluminum that $\omega_p = 2.24 \times 10^{16}$, $\gamma = 1.22 \times 10^{14}$ and $\varepsilon_\infty = 1$ [16]. The power transmission of the structure versus normalized frequency at normal incidence is plotted in Fig. 8. In this figure, dashed line represents the results obtained by rigorous approached of [13], [14], and solid line shows the results of the proposed circuit model. It is obvious from this figure that the proposed model is fairly accurate in the visible range $(1.33 < \omega_n < 2.63)$ (399 THz $< f <$ 789 THz). Therefore,

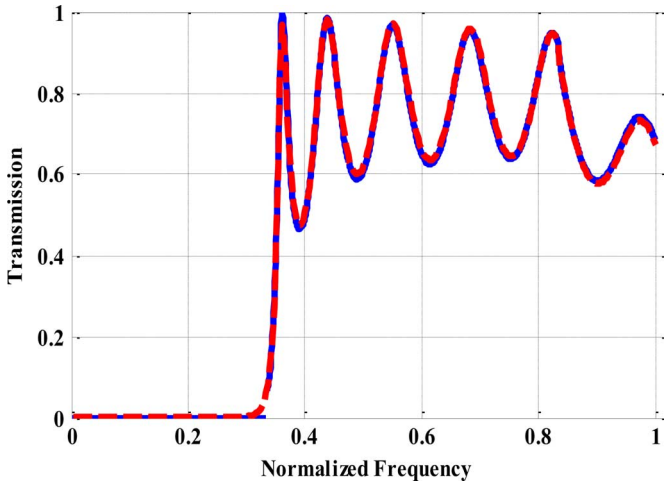


Fig. 9. Transmitted power through a grating illuminated by a TE polarized incident plane wave versus normalized frequency calculated by the rigorous approach of [13], [14] (dashed line), proposed circuit model (solid line). The structure parameters are: $n_1 = 1.2, n_2 = 2, n_3 = 3, d = 200\ \mu$m, $a = 150\ \mu$m, and $h = 300\ \mu$m. The grating is under normal incidence.

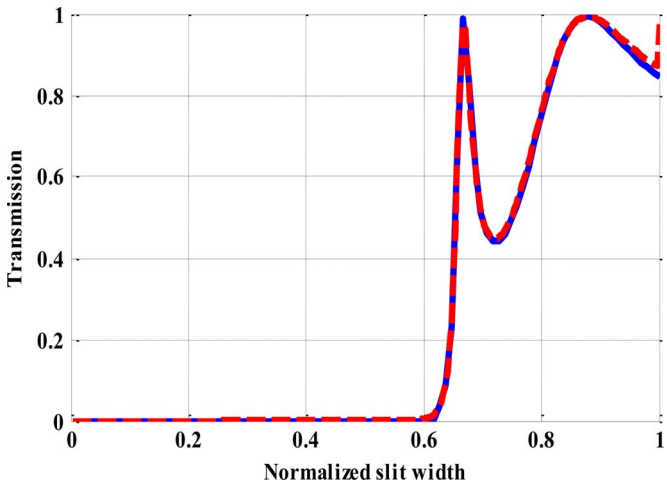


Fig. 10. Transmitted power through a grating illuminated by a TE polarized incident plane wave versus normalized slit width calculated by the rigorous approach of [13], [14] (dashed line), proposed model (solid line). The grating parameters are: $n_1 = 1.2, n_2 = 2, n_3 = 3, d = 200\ \mu$m and $h = 300\ \mu$m. The normalized frequency is $\omega_n = 0.4$. The grating is under normal incidence.

the proposed model can be used in this range and it can successfully explain the EOT.

The final example verifies the accuracy of the proposed model for TE polarization. In Fig. 9, we have plotted the power transmission of the structure shown in Fig. 1(a) versus normalized frequency at normal incidence with consideration of all diffracted orders. The structure parameters are: $n_1 = 1.2, n_2 = 2, n_3 = 3, d = 200\ \mu$m, $a = 150\ \mu$m, and $h = 300\ \mu$m. In Fig. 9, the dashed line shows rigorous full-wave simulations, and the solid line represents the result obtained by the proposed circuit model. Since higher modes are excited inside the slits at higher frequencies, we restrict ourselves to the frequency range of 0–1.5 THz.

We also plot the transmission of the previous example versus the incident angle and normalized slit width in Figs. 10 and 11, respectively. In these two figures, the normalized frequency is set to $\omega_n = 0.4$ ($f = 0.6$ THz).

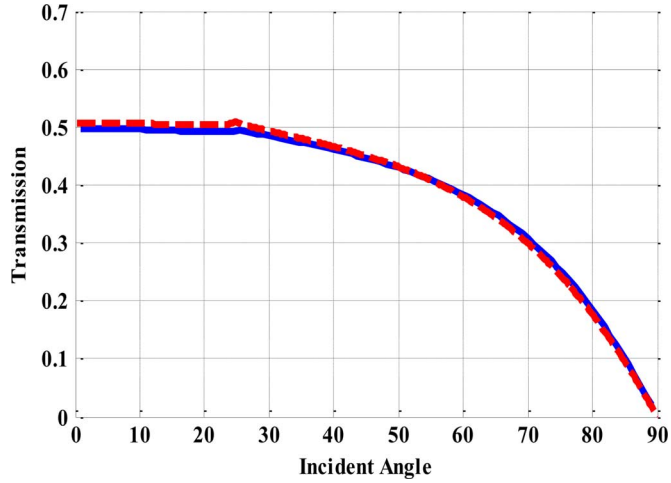


Fig. 11. Transmitted power through a grating illuminated by a TE polarized incident plane wave versus incident angle calculated by the rigorous approach of [13], [14] (dashed line) and the circuit model (solid line). The grating parameters are: $n_1 = 1.2, n_2 = 2, n_3 = 3, d = 200\ \mu$m, $a = 150\ \mu$m, and $h = 300\ \mu$m. The normalized frequency is $\omega_n = 0.4$.

## V. Conclusion

In conclusion, we proposed an equivalent circuit model for modeling one-dimensional periodic array of metallic slits which is valid even for wavelength smaller than the period of the structure. The proposed model is obtained by assuming only one guided mode inside the slits. Furthermore, it was assumed that all diffracted orders can be propagating; consequently, in TM polarization, the proposed circuit model consists of infinite number of parallel capacitors, each representing a specific diffracted order. The capacitance of the mentioned capacitors has been given by an analytical expression. We have been shown that when a higher diffracted order becomes propagating, its equivalent capacitor converts to a resistor and the power dissipated in each resistor is equal to the power transmitted to its corresponding diffracted order.

The model was also extended to the TE polarization and it was demonstrated that the capacitors should be replaced by inductors.

The simulation results of the introduced circuit model are in almost complete agreement with those obtained by a rigorous method. It was also shown that the proposed model is valid from very low frequencies up to the visible range.

## References

[1] T. W. Ebbesen, H. J. Lezec, H. F. Ghaemi, T. Thio, and P. A. Wolff, "Extraordinary optical transmission through sub-wavelength hole arrays," *Nature*, vol. 391, pp. 667–669, Feb. 1998.

[2] A. Khavasi and K. Mehrani, "Circuit model for lamellar metallic gratings in the sub-wavelength regime," *IEEE Trans. Quantum Electron.*, vol. 43, no. 10, pp. 1330–1335, Nov. 2011.

[3] K. Yee, "Numerical solution of initial boundary value problems involving Maxwell's equations in isotropic media," *IEEE Trans. Antennas Propag.*, vol. AP-14, no. 3, pp. 302–307, May 1966.

[4] T. Weiland, "A discretization method for the solution of Maxwell's equations for six- component fields," *Electron. Commun.*, vol. 31, pp. 116–120, 1977.

[5] F. Medina, F. Mesa, and R. Marques, "Extraordinary transmission through arrays of electrically small holes from a circuit theory perspective," *IEEE Trans. Microw. Theory Tech.*, vol. 56, no. 12, pp. 3108–3120, Dec. 2008.

[6] A. Khavasi, M. Edalatipour, and K. Mehrany, "Circuit model for extraordinary transmission through periodic array of subwavelength stepped slits," *IEEE Trans. Antennas Propag.*, vol. 61, no. 4, pp. 2019–2024, Apr. 2013.
[7] F. Medina, F. Mesa, and D. C. Skigin, "Extraordinary transmission through arrays of slits: A circuit theory model," *IEEE Trans. Microw. Theory Tech.*, vol. 58, no. 1, pp. 105–115, Jan. 2010.
[8] R. Rodriguez-Berral, F. Medina, and F. Mesa, "Circuit model for a periodic array of slits sandwiched between two dielectric slabs," *Appl. Phys. Lett.*, vol. 96, no. 16, p. 1104(3), Apr. 2010.
[9] R. Yang, R. Rodriguez-Berral, F. Medina, and Y. Hao, "Analytical model for the transmission of electromagnetic waves through arrays of slits in perfect conductors and lossy metal screens," *J. Appl. Phys.*, vol. 109, May 2011.
[10] D. K. Cheng, *Field and Wave Electromagnetics*. New York, NY, USA: Addison-Wesley, 1989.
[11] M. G. Moharam, E. B. Grann, and D. A. Pommet, "Formulation for stable and efficient implementation of the rigorous coupled-wave analysis of binary gratings," *J. Opt. Soc. Amer. A*, vol. 12, no. 5, pp. 1068–1076, May 1995.
[12] S. A. Maier, *Plasmonics Fundamentals and Applications*. New York, NY, USA: Springer, 2007.
[13] A. Khavasi and K. Mehrany, "Adaptive spatial resolution in fast, efficient, and stable analysis of metallic lamellar gratings at microwave frequencies," *IEEE Trans. Antennas Propag.*, vol. 57, no. 4, pp. 1115–1121, Apr. 2009.
[14] A. Khavasi and K. Mehrany, "Regularization of jump points in applying the adaptive spatial resolution technique," *Opt. Commun.*, vol. 284, no. 13, pp. 3211–3215, 2011.
[15] G. Granet, "Reformulation of lamellar grating problem through the concept of adaptive spatial resolution," *J. Opt. Soc. Amer. A*, vol. 16, no. 10, pp. 2510–2516, Oct. 1999.
[16] M. A. Ordal, L. L. Long, R. J. Bell, S. E. Bell, R. R. Bell, R. W. Alexander, Jr., and C. A. Ward, "Optical properties of the metals Al, Co, Cu, Au, Fe, Pb, Ni, Pd, Pt, Ag, Ti, and W in the infrared and far infrared," *Appl. Opt.*, vol. 22, no. 7, pp. 1099–1119, Apr. 1983.

**Elahe Yarmoghaddam** was born in Tehran, Iran, on July 7, 1990. She received the B.Sc. degree in electrical engineering from the Sharif University of Technology, Tehran, Iran, in 2012. She is currently pursuing the M.Sc. degree with the same university.

Her current research interests include photonics, circuit modeling of photonic structures, and plasmonics.

**Ghazaleh Kafaie Shirmanesh** was born in Tehran, Iran, on March 22, 1990. She received the B.Sc. degree in electrical engineering from the Sharif University of Technology, Tehran, Iran, in 2012. She is currently pursuing the M.Sc. degree with the same university.

Her current research interests include photonics, circuit modeling of photonic structures, and plasmonics.

**Amin Khavasi** was born in Zanjan, Iran, on January 22, 1984. He received the B.Sc., M.Sc., and Ph.D. degrees in electrical engineering from the Sharif University of Technology, Tehran, Iran, in 2006, 2008, and 2012, respectively.

He has been an Associate Professor with the Department of Electrical Engineering, Sharif University of Technology, since 2013. His current research interests include photonics, circuit modeling of photonic structures, and computational electromagnetics.

**Khashayar Mehrany** was born in Tehran, Iran, on September 16, 1977. He received the B.Sc., M.Sc., and Ph.D. (magna cum laude) degrees in electrical engineering from the Sharif University of Technology, Tehran, in 1999, 2001, and 2005, respectively.

He has been an Associate Professor with the Department of Electrical Engineering, Sharif University of Technology, since 2005. His current research interests include photonics, semiconductor physics, nanoelectronics, and numerical treatment of electromagnetic problems.